JACS Au
AN OPEN ACCESS JOURNAL OF THE AMERICAN CHEMICAL SOCIETY

pubs.acs.org/jacsau

Article

Descriptor and Scaling Relations for Ion Mobility in Crystalline Solids

Mohsen Sotoudeh* and Axel Groß*

Cite This: *JACS Au* 2022, 2, 463−471

Read Online

ACCESS | Metrics & More | Article Recommendations | Supporting Information

ABSTRACT: Ion mobility is a critical performance parameter not only in electrochemical energy storage and conversion but also in other electrochemical devices. On the basis of first-principles electronic structure calculations, we have derived a descriptor for the ion mobility in battery electrodes and solid electrolytes. This descriptor is entirely composed of observables that are easily accessible: ionic radii, oxidation states, and the Pauling electronegativities of the involved species. Within a particular class of materials, the migration barriers are connected to this descriptor through linear scaling relations upon the variation of either the cation chemistry of the charge carriers or the anion chemistry of the host lattice. The validity of these scaling relations indicates that a purely ionic view falls short of capturing all factors influencing ion mobility in solids. The identification of these scaling relations has the potential to significantly accelerate the discovery of materials with desired mobility properties.

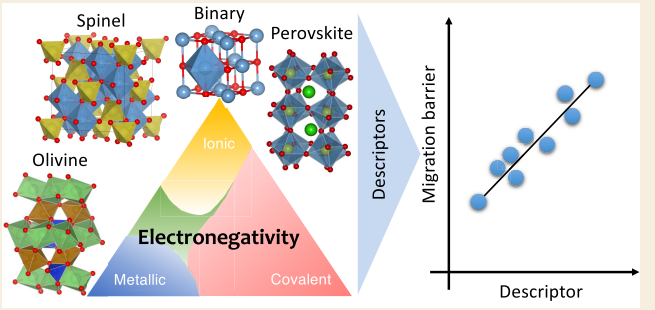

KEYWORDS: *ion conductivity, migration barriers, density functional theory, battery electrodes, solid electrolytes, descriptor, electronegativity, scaling relations*

INTRODUCTION

Electrochemical energy storage devices play a central role in our attempts toward decarbonization through the storage of volatile renewable energy and the emission-free usage of vehicles and mobile devices. Significant progress has been made in this respect due to the development of advanced Li-ion battery technologies.[1,2] In addition, recently so-called post-Li-ion technologies[3,4] have drawn a great deal of attention in order to address, among others, sustainability issues associated with the materials typically used in Li-ion batteries.[5,6] In post-Li-ion batteries, other charge carriers such as monovalent Na and K cations[7,8] and divalent Mg and Ca cations[9−13] are used. These post-Li-ion batteries, in particular those based on multivalent ions, can compete with existing Li-ion batteries or even outperform them, as far as energy density and safety are concerned,[14,15] the latter in particular with respect to their lower tendency for dendrite growth.[16−20] Furthermore, as liquid electrolytes are prone to corrosion processes and often represent fire hazards because of their flammability, all-solid-state batteries with higher safety and better electrochemical stability[21] based on materials such as inorganic oxides,[22,23] hydrides,[24−26] and chalcogenides[27,28] have been intensely studied for all possible charge carriers.

A critical parameter that significantly influences the performance of batteries is the ion mobility both in the electrolyte and in the electrodes.[29−31] In particular, batteries based on multivalent ions such as Mg^{2+} are plagued with low ion mobility[32−34] due to their stronger interaction with the host structures in comparison to monovalent ions such as Li^{+}. Hence, the identification and development of materials with improved ion mobility are essential for more efficient electrochemical energy storage devices. However, ion conduction in solids is important not only in battery materials but also in many other applications such as, e.g., solar cells.[35]

A very useful concept in order to accelerate materials discovery is based on so-called descriptors.[36,37] They represent fundamental materials properties or combinations thereof that are correlated with a desired or undesired functionality of the material. This concept has been very successfully used not only in heterogeneous catalysis,[38] in particular in connection with so-called scaling relations,[39] but also already in battery research.[20] The identification of descriptors can significantly speed up the search for new materials with the desired functional properties because, once they are identified, only the particular descriptors need to be optimized in a first step. Thus, promising candidate materials can be proposed whose properties can then be scrutinized in detail.

Received: November 9, 2021
Published: February 11, 2022

In fact, also with respect to ion mobility in solids, a number of possible descriptors have been proposed on the basis of, e.g., the lattice volume and ionic size,[28,29] the choice of the anion sublattice,[29,40] the lattice dynamics,[29,41,42] or the preferred crystal insertion site.[30] However, many of the identified descriptors are restricted to some particular crystal structure. Furthermore, some are based on materials properties that are not easily accessible. Hence, it is fair to say that so far no convenient descriptor has been established that is able to predict ion mobility across a set of different structures.

On the basis of the results of first-principles density functional theory (DFT) calculations and physicochemical reasoning, here we propose such a convenient descriptor for the ion mobility, the so-called migration parameter or number, which is based on the product of Pauling's electronegativity, ionic radii, and oxidation states of the involved compounds, all properties that are easily accessible for any material. This particular descriptor, whose choice is also supported by a statistical analysis of our first-principles results, goes beyond current proposals by also considering deviations from a purely ionic interaction between the migrating ion and the host lattice. According to our calculations, the activation barrier for migration is connected to this migration number via linear scaling relations within particular materials classes. This allows the prediction of the activation barriers both for the variation of the cation chemistry of the migrating ion and for the variation of the anion chemistry of the host lattice. Thus, this descriptor will most probably significantly accelerate the discovery of materials with favorable mobility properties. As this migration number is based on basic physicochemical quantities, it also enables a deeper fundamental understanding of the principles underlying ion mobility.

RESULTS AND DISCUSSION

From a microscopic viewpoint, migration or diffusion in solid crystalline materials occurs by atomic hops in a lattice. Such jump processes are typically thermally activated, and the corresponding tracer diffusion coefficient is given by

$$D^{\mathrm{tr}} = D_0^{\mathrm{tr}} \exp\left(-\frac{E_a}{k_B T}\right) \quad (1)$$

Here D_0^{tr} is the pre-exponential factor, k_B the Boltzmann constant, and T the absolute temperature. E_a is the activation barrier corresponding to the energy barrier along the minimum energy path connecting two equivalent intercalation sites, as illustrated in Figure 1. Such a minimum energy path can be determined by automatic search routines.[43] In the present work, we have used the nudged elastic band (NEB) method[44] in the DFT calculations to derive the activation barrier E_a. The electronic structure calculations were performed using the Vienna *ab initio* simulation package (VASP)[45] employing the projector augmented wave (PAW)[46] method with the exchange-correlation effects being described with the Perdew–Burke–Ernzerhof (PBE) functional.[47] This functional has been used in order to avoid the well-known problems in obtaining converged NEB results when more advanced approaches are used. In fact, this approach is sufficient to yield reliable structural properties and thus the migration barriers for the compounds addressed in this study, as shown below, except for the exact size of the band gap.

Note that in general we have performed the calculations for charge-neutral cells. This is the correct approach for battery electrodes, as upon charge and discharge atoms and not ions will be transferred. The same is true for solid electrolytes, which are also called single-ion conductors[48] where the "counterion" is provided by the charge distribution within the host lattice. As far as the binary compounds are concerned, the charge of, say, anion vacancies is typically compensated by a corresponding amount of cation vacancies. In order to model this adequately, we added a compensating charge background, as has been done before,[49] to ensure that our model retains charge neutrality while not exhibiting major structural distortions. Further details about the DFT calculations are provided in the Supporting Information.

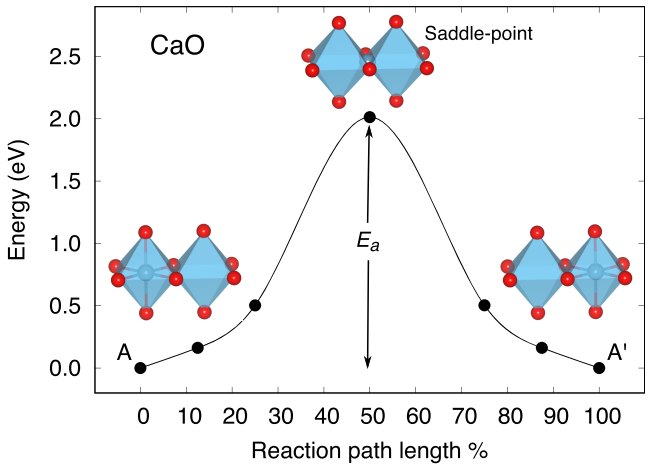

Figure 1. Illustration of a cation interstitial migration mechanism, using Ca diffusion in CaO as an example. A diffusion event corresponds to the migration of the Ca cation from the energetically most favorable octahedral site A to the nearest equivalent site A′ through the transition state which corresponds to a saddle point in the multidimensional potential energy surface and which can be derived by first-principles electronic structure calculations. The activation energy or diffusion barrier is denoted by E_a, which corresponds to the energy difference between the saddle point and the initial configuration.

Motivated by the goal to identify the fundamental factors determining ion mobility in solids, in a previous study[28] we had derived the activation barriers for the diffusion of a number of ions of varying size and charge in the same host lattice, a chalcogenide spinel. We obtained the expected results: namely, that the size and the charge of the diffusing ion matter. However, the ionic radius of the charge carrier alone could not explain the observed trends but rather the distance between the ion in the tetrahedral site and the nearest chalcogenide atom. In order to further elucidate the mobility-determining factors, we decided to look at structurally simpler compounds, namely binary A_nX_m materials with A being the migrating ion. In total, we looked at 35 different compounds with Li, Mg, and Ca as the migrating ion A.

For these binary materials, we again found that the size and charge of the propagating ions matter, but not in a very systematic way, as has already been observed by others.[29] However, we recently could show that the stability of ions in chalcogenide spinels can only be understood if deviations from a purely ionic interaction are taken into account.[50] It is essential to realize that the considered binary materials span the whole range of interaction characteristics between metallic and ionic bonding. Such bonding characteristics can in fact been classified in so-called Van Arkel–Ketelaar triangles,[51] in which compounds are placed according to the mean electronegativity $\chi_{\mathrm{mean}}(x \text{ axis})$ and the electronegativity difference $\Delta\chi(y \text{ axis})$ of the constituting elements.

https://doi.org/10.1021/jacsau.1c00505
JACS Au 2022, 2, 463–471

Figure 2a shows the Van Arkel–Ketelaar triangle including the Mg binary compounds considered in this study. A large

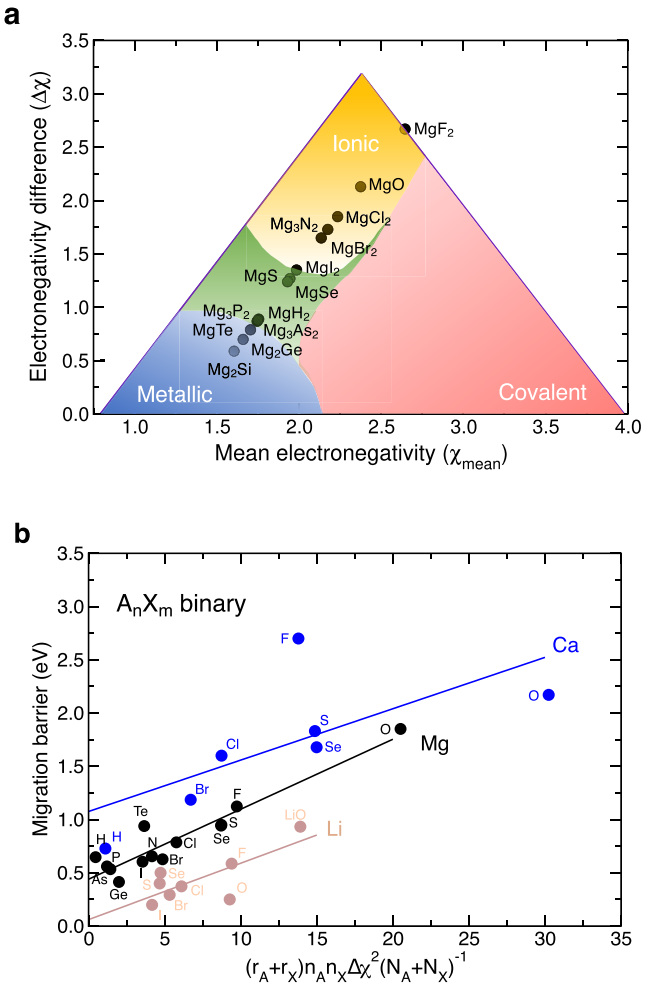

Figure 2. A_nX_m binaries considered in this study. (a) Van Arkel–Ketelaar triangle with the considered Mg_nX_m binaries plotted as a function of the mean electronegativity and the difference in the electronegativity of the two components. (b) Calculated activation energies for the migration of A = Li, Mg, Ca in A_nX_m binaries as a function of the migration number N_{migr}^{AX} for various elements X according to eq 2. The solid lines correspond to linear regressions of these results.

difference in electronegativity indicates ionic bonding characteristics (shown in yellow), as are present in MgO and MgF_2. CsF (not shown) would lie at the apex of the triangle. At the bottom of the triangle, corresponding to a vanishing electronegativity difference, an increasing mean electronegativity is associated with more directional bonding. Hence, the lower right corner gathers covalent systems whereas the lower left corner contains metallic systems.

The Mg_nX_m binaries considered in this study all fall along a line between metallic and ionic bonding, which is based on the fact that the cation in the binaries, Mg^{2+}, has not been varied. In detail, MgF_2 has the highest electronegativity difference $\Delta\chi$, indicating a strong ionic bond. This is also true for MgO, whereas Mg_2Si is associated with the lowest value of $\Delta\chi$ demonstrating metallic bonding. The remaining compounds, Mg halides, Mg chalcogenides, Mg pnictides, and Mg tetrels, are located between strongly ionic and metallic bonding, as indicated by the green area. They are divided into three groups. $MgCl_2$, $MgBr_2$, and Mg_3N_2 are characterized by a large electronegativity difference of about 1.7, demonstrating a predominantly ionic bonding (light yellow region). MgI_2, MgS, and MgSe have $\Delta\chi \approx 1.3$, and the other Mg binaries have electronegativity differences below 1.

By a summary of the discussion above, it appears to be evident that the charges of the migrating ion and of the ion of the host lattice n_A and n_X and their ionic radii r_A and r_X, respectively, are all decisive factors for the height of the migration barriers. An increase in any of these quantities typically raises this barrier. Therefore, we decided that the product of these quantities should enter a possible descriptor for the height of the migration barriers. However, in a previous study[28] we found that the distance of the ions is the crucial parameter influencing the barrier heights, which can be represented by the sum $r_A + r_X$ of their ionic radii. Furthermore, in another previous study[50] we have demonstrated that purely ionic concepts are not sufficient to understand the properties of nominally ionic crystals. Consequently, for the crucial new ingredient in the identification of a possible descriptor we propose to quantify the degree of the ionicity of the interaction through the square of the difference in the electronegativities of the migrating cation and the anion of the host lattice. As the barriers increase with a higher ionicity, this square should enter the descriptor as another multiplicative factor. This allows us to quantify the notion of hard and soft anions, which is typically only discussed in a qualitative fashion. Altogether, these arguments motivated us to define the *migration* parameter or number N_{migr}

$$N_{migr}^{AX} = (r_A + r_X)n_A n_X \Delta\chi_{AX}^2/(N_A + N_X) \quad (2)$$

as the product of these three quantities, where the ionic radii r_A and r_X are given in Å and n_A and n_X are the absolute values of the formal integer oxidation states or numbers. Note that all the parameters entering our proposed descriptor are readily available and easily accessible so that that there is no need to determine specific parameters before applying our descriptor. We tried several alternative algebraic operations to combine these materials features, and the multiplication turned out to be the optimal choice, indicating that an increase in any of these three features leads to a larger migration number.

In addition, also the number of atoms of the corresponding species in the unit cell of the crystal N_A and N_X enters through their sum in the denominator. In Figure 2b, we plot the dependence of the migration barriers as a function of the migration parameter for the three migrating ions Li, Mg, and Ca in the low-vacancy limit. The low-vacancy limit has been realized by removing just one migrating cation within the supercell, resulting for example in a $Ca_{0.97}O$ stoichiometry for calcium oxide. In spite of some outliers, overall the migration barriers nicely follow separate scaling relations for each migrating ion

$$\begin{aligned} E_a^A(X) &= E_0^A + C^A(r_A + r_X)n_A n_X \Delta\chi_{AX}^2/(N_A + N_X) \\ &= E_0^A + C^A N_{migr}^{AX} \end{aligned} \quad (3)$$

as a function of the migration number N_{migr}^{AX} for the A-site vacancy diffusion, where C^A presents the slope of the straight line and E_0^A is the energy that corresponds to the intercept at the y axis. These last two parameters are not predicted by our model but need to be derived from a linear regression of the results.

The presence of universal scaling relations strongly suggests that the same factors govern the ion mobility in all considered

https://doi.org/10.1021/jacsau.1c00505
JACS Au 2022, 2, 463–471

binary compounds. It is no surprise that there are a few outliers indicating that other critical contributions to the activation energies can play a role: for example, Coulomb interactions beyond those represented by the oxidation states, quantum mechanical overlap effects, and polarization.[29] For example, the most prominent outlier in Figure 2b corresponds to CaF_2. This binary compound combines the element with the highest electronegativity, fluorine, with an element with a rather small electronegativity. Furthermore, interestingly enough F^- and Ca^{2+} have very similar ionic radii, 1.19 and 1.14 Å, respectively. Still, the migration number yields a barrier that is too small by about 1 eV. At this point, we can only speculate about the reasons for this deviation; however, a strong ionic interaction could belong to the characteristics of the compounds that would lead to an outlier. However, the reason might also lie in the unusual properties of CaF_2, which as a molecule is quasi-linear, meaning that its nuclear potential is very flat along the bending coordinate.[52]

In order to verify that we still identified the crucial parameters governing ion mobility in these binary materials, we applied a statistical compressed-sensing approach using the sure-independence screening and sparsifying operator SISSO,[53] as described in detail in the Supporting Information, to search for possible descriptors. We used the following input parameters or so-called primary features: number of atoms in the unit cell (N_{atom}) and the atomic masses of the two elements in the binary compound (m_A, m_X), their formal oxidation numbers (n_A, n_X) and ionic radii (r_A, r_X), the Pauling electronegativity (χ_A, χ_X) of both elements, the A−X bond distances d_{A-X}, and the unit cell volume V. This approach allows us to vary the dimensionality Ω of the descriptor space, and the descriptor is expressed as a linear combination of so-called features that are nonlinear functions of the input parameter or primary features. For $\Omega = 1$, we obtained the descriptor

$$d = ((n_X/n_A) - \cos n_X)/(\chi_X^6 \sin m_X) \quad (4)$$

whereas for $\Omega = 2$ we found a two-dimensional descriptor consisting of the two features d_1 and d_2:

$$d_1 = n_X^2 \times (r_{Mg} + r_X) \quad (5)$$

$$d_2 = \chi_X^3/N_{atom} \quad (6)$$

Indeed, these findings confirm that the oxidation states reflecting the charge of the atoms, the ionic radii, and the electronegativity differences are the determining factors for the migration barriers. Interestingly, the unit cell volume V, which has been shown to substantially influence the ionic mobility in some structural families,[28,29] does not show up in these statistically derived descriptors. However, note that the functional dependences found by the SISSO operators do not allow for a straightforward interpretation of the physicochemical factors underlying the migration process. For example, in our migration parameter given in eq 2, the absolute values of the oxidation states enter as multiplicative parameters, reflecting the fact that more highly charged species interact more strongly with the environment, which thus increases the migration barriers. In contrast, in the descriptor d according to eq 4, the oxidation states enter as $(n_X/n_A) - \cos n_X$, which is hard to interpret. Note that in fact the migration number N_{migr} also outperforms the one-dimensional SISSO descriptor d. The RMSE (root mean square error) for the 1D SISSO descriptor d is 0.183 eV, whereas the corresponding RMSE associated with the migration number N_{migr} is only 0.113 eV.

Therefore, we decided to look for a verification of whether the observed scaling relations as a function of the migration parameter (eq 2) are also valid for other material types. As this study was originally motivated by the results for migration barriers of A^{n+} in AB_2X_4 spinel structures, we reconsidered our previous results.[28] For these structures, the NEB method was again applied in the low-vacancy limit. In Figure 3, we have

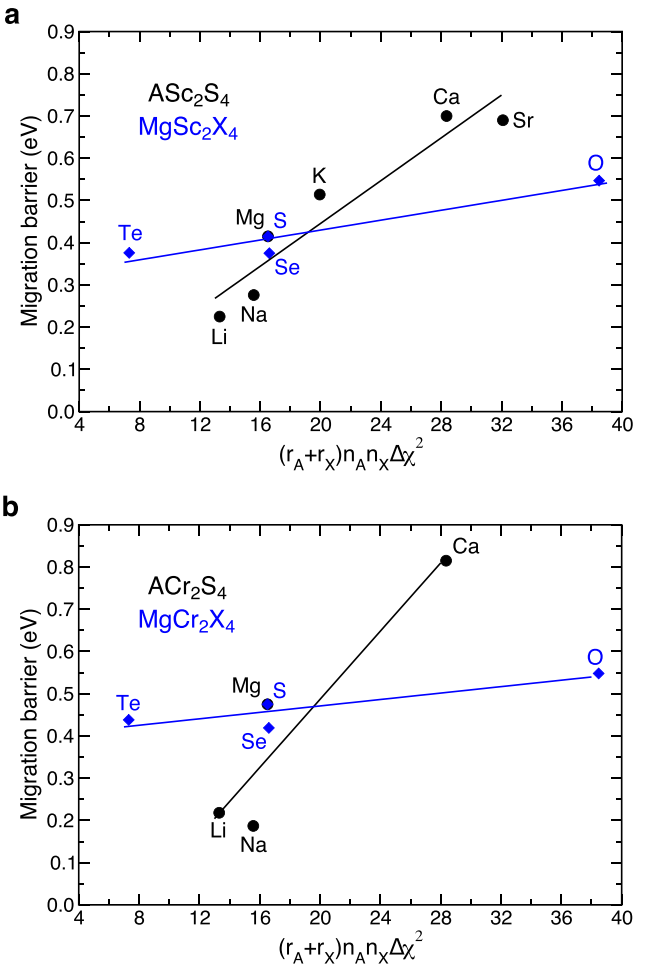

Figure 3. (a) Migration barriers (in eV) in ASc_2X_4 as a function of the migration parameter $(r_A + r_X)n_An_X\Delta\chi_{AX}^2$ (eq 2) for ASc_2S_4 (black symbols) and $MgSc_2X_4$ spinels (blue symbols) for various mono- and multivalent cations A^{n+} and anions X^{n-}. (b) The same as in (a), but with Sc replaced by Cr.

plotted the migration barriers E_a (in eV) as a function of the migration parameter given in eq 2 for ASc_2S_4 and $MgSc_2X_4$ spinels (Figure 3a) and ACr_2S_4 and $MgCr_2X_4$ spinels (Figure 3b), respectively. Note that the factor $1/(N_A + N_X)$ has been omitted in the definition of the x axis, as this factor is constant for all considered materials. Again, as in Figure 2, we find a linear scaling of the migration barriers upon variation of the anions X^{n-} (blue symbols). Interestingly enough, we also find additional scaling relations upon variation of the cations Li^+, Na^+, K^+, Mg^{2+}, Ca^{2+}, and Sr^{2+} (black symbols) (note that the $MgSc_2S_4$ and $MgCr_2S_4$ spinels, respectively, are part of both corresponding subsets). These results demonstrate that the scaling relations given in eq 3 are independently valid for the variation of either

https://doi.org/10.1021/jacsau.1c00505
JACS Au 2022, 2, 463−471

the cation chemistry of the migrating ions A^{n+} or the variation of the anion chemistry of the host lattice ions X^{n-}.

As far as the comparison of our calculated migration barriers with the experiments is concerned, one has to consider that their experimental determination is not trivial. Consequently, only a few experimental results are available. However, our calculated barrier height for the spinel selenide $MgSc_2Se_4$ of 0.375 eV agrees within 10 meV with the experimental value of 0.37 ± 0.09 eV.[27] Furthermore, for the spinel oxides $MgCr_2O_4$ and $MgMn_2O_4$, experimental barrier heights of 0.62 ± 0.10 and 0.70 ± 0.05 eV, respectively, are found,[54] whereas we obtain DFT-PBE values of 0.54 and 0.73 eV. This nice agreement between experimentally and theoretically obtained barrier heights lends credibility to the reliability of our computational approach.

As Figure 3 illustrates, upon variation of the host lattice cations B^{n+} present in the sulfide spinels AB_2X_4, which are typically transition-metal cations, the slope of the linear scaling relations represented by the parameter C^A in eq 2 changes. We have determined the height of the migration barriers for the six additional transition metals B = Ti, V, Mn, Fe, Co, Ni as a function of the migration number upon variation of the migrating cations A^{n+} and collected the results in Figure 4. We

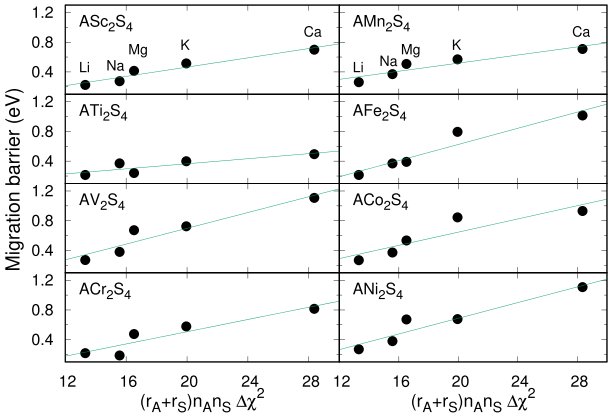

Figure 4. Migration barriers (in eV) in AB_2S_4 spinels as a function of the migration number N_{migr}^{AS} for eight different transition metal cations B = Sc, Ti, V, Cr, Mn, Fe, Co, Ni upon variation of migrating cations A = Mg, Na, K, Mg, Ca.

again find that the migration barriers follow linear scaling relations, but with different slopes. It is interesting to note that the difference $\Delta E_a^A(B)$ between the lowest and the highest migration barriers upon variation of the eight considered transition metals B increase with the size and charge of the migrating cations A^{n+}, as can be derived from the values of $\Delta E_a^A(B)$ given in Table 1. Apparently, for increasing charge and size of the host lattice cations B, the specific nature of the

Table 1. Difference $\Delta E_a^A(B)$ in eV between the Lowest and the Highest Migration Barrier for the Charge Carriers A = Li, Na, K, Mg, Na in AB_2X_4 Spinels upon Variation of the Eight Considered Transition Metals B Shown in Figure 4

	migrating ion				
	Li^+	Na^+	K^+	Mg^{2+}	Ca^{2+}
$\Delta E_a^A(B)$ (eV)	0.08	0.19	0.42	0.44	0.61

interaction between the cations A and B becomes more prominent, as far as the migration barriers for A are concerned. Of particular interest is that we find a higher slope for transition metals V, Fe, Co, and Ni as the metal cation B in the spinels. As multivalent ions are associated with higher migration numbers, this means that these transition metals are not favorable for the migration of multivalent ions. In contrast, the transition metals Ti, Mn, and Sc lead to a reduced slope, showing the potential of the respective spinel materials for being good multivalent ion conductors.

Note that in the migration number N_{migr}^{AX} (eq 2), parameters of the migrating cations A and of the anions X of the host lattice enter. However, in the spinels AB_2X_4 there are also further cations B^{n+} present, typically transition-metal cations, that are not considered in the migration number but which should also be of significance in the A ion transport. In these materials, the B−X bond is dominantly covalent. In Figure 5, we have plotted

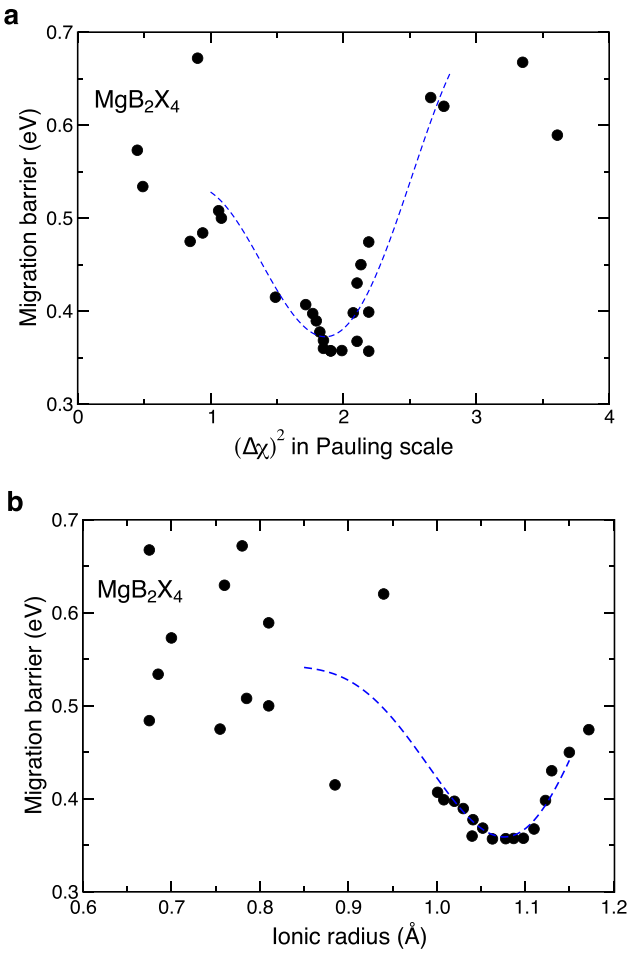

Figure 5. Mg migration barriers (in eV) as a function of (a) the squared electronegativity difference between transition metal B and anion X and (b) the ionic radius of the transition metal B for a number of MgB_2X_4 spinels.

migration barriers for MgB_2X_4 spinels as a function of the squared electronegativity difference between transition metal B and anion X (Figure 5a) and the ionic radius of the transition metal B (Figure 5b) for a number of MgB_2X_4 spinels. Note that there is some scatter in the data. However, there is a clear minimum in the height of the migration barriers in Figure 5a for values of $\Delta\chi^2 \approx 2$. Furthermore, the unit-cell volume of the

https://doi.org/10.1021/jacsau.1c00505
JACS Au 2022, 2, 463−471

spinel increases by substituting a larger B cation into the structure. Again we find a clear minimum in the height of the migration barriers in Figure 5b, here for the ionic radius of the transition metal B at values of $r_B \approx 1.1$ Å. These findings reflect that also the choice of the B cations plays a role in minimizing the ion migration barriers in the spinel compounds, in contrast to previous theoretical conclusions[30] which were, however, based on a much smaller number of studied systems.

Still, we did not manage to identify any linear scaling relations upon the variation of the cation B. On the basis of the identification of these pronounced minima and the corresponding matching properties of Zr, we identified $MgZr_2S_4$ as a promising ion conductor with a high ion mobility, and indeed we found that $MgZr_2S_4$ has a rather low Mg migration barrier of only 0.3 eV.

In order to demonstrate the versatility and reliability of our proposed descriptor, we have applied the concept to two further classes of materials that are also of interest as battery materials. We have chosen the olivine $AFeSiO_4$, which has been considered as a promising cathode material,[55] and the perovskite $AMnO_3$, which has been suggested as a possible anode material.[56] Cation migration barriers in the olivine $AFeSiO_4$ and in the perovskite $AMnO_3$ are shown in Figure 6a,b, respectively, as a function of the migration parameter $(r_A + r_O)n_An_O\Delta\chi^2_{AO}$ (eq 2) for varying charge carriers A. Note that again a convincing linear scaling relation has been obtained for these two additional materials classes.

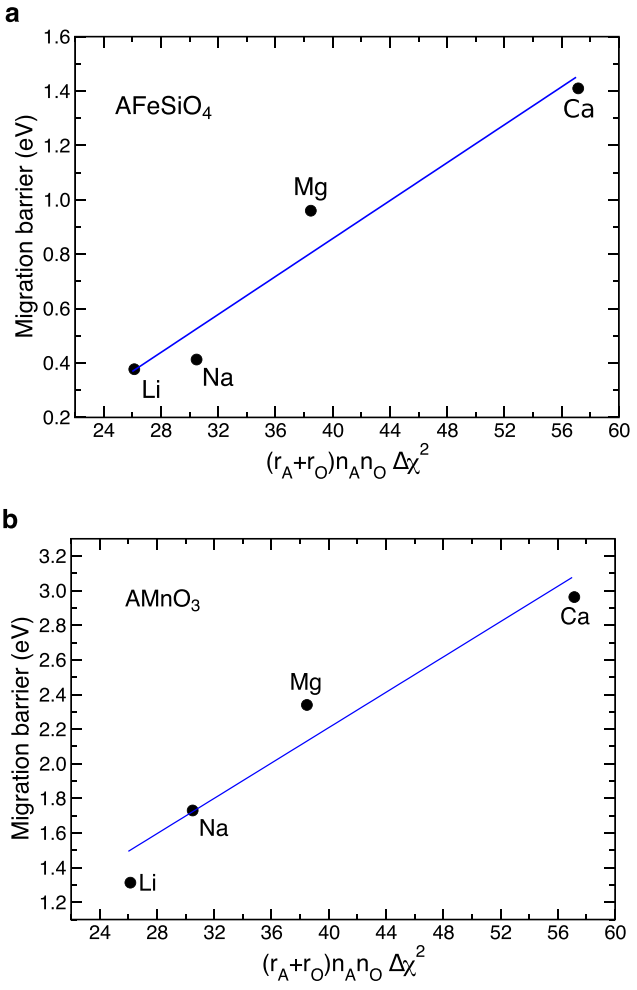

Figure 6. Migration barriers (in eV) in the olivine $AFeSiO_4$ (a) and in the perovskite $AMnO_3$ (b) as a function of the migration parameter $(r_A + r_O)n_An_O\Delta\chi^2_{AO}$ (eq 2) for varying charge carriers A.

The fact that the migration parameter N^{AX}_{migr} captures the essence of the migration barrier height upon variation of the migrating cation A and the anion X of the host lattice calls for a critical assessment of this parameter. There are some obvious factors influencing the height of the migration barrier. For larger ions it will be harder to migrate through a given lattice; therefore, it is no surprise that the ion radius r_A enters the migration barrier. However, when the size of the anion of the host lattice is also varied, it becomes apparent that it is the size of both the cation and the anion represented by $r_A + r_X$ that is the critical length parameter, as was already stressed in a previous study.[28] Furthermore, note that in many cases the dependence of the mobility on the ionic radius is not monotonic;[29] thus, any descriptor of the ion mobility taking into account the ionic radius needs to reflect this nonmonotonic behavior.

It is also well-known that the charge of the migrating ion matters with respect to the ion mobility. The higher the charge of an ion, the stronger its interaction with the environment and thus the higher the migration barriers. This same argument of course also applies to the charge of the ions constituting the host lattice, as the ionic interaction scales with the product of the charges of interacting ions. These charges enter the migration parameter through the product of the oxidation numbers n_An_X.

However, it is important to realize that in the migration of "ions" in a host lattice it is not *a priori* clear that the "ions" keep their ionic charge. Any crystal containing migrating ions has to be overall charge neutral because macroscopically charged matter is unstable. Hence, any charge on the migrating ions has to be compensated by the host lattice. Of course, the assumption that strong ions remain charged in a host lattice makes a lot of sense and is the basis of the concept of formal oxidation numbers. Still, formal atomic charges in a material are not good observables because it can not be uniquely defined which electrons belong to the migrating ion and which belong to the host lattice, as the electrons are shared between the bonding partners. This is also the reason why there is a broad variety of different charge partition schemes[57−60] used in quantum chemical codes in order to derive atomic charge numbers, which can give quite different quantitative results. Furthermore, there are hardly any chemical systems in which the interaction is purely ionic, purely covalent, or purely metallic. Therefore, it is not surprising that trends in the ion mobility cannot be fully understood on the basis of formal oxidation states alone.

This deviation from the purely ionic interaction can be characterized by the difference in the electronegativity $\Delta\chi^2$ of the interacting compounds, which is also the basis for the Van Arkel−Ketelaar triangle. In this context it should be noted that the Pauling electronegativity in the form revised by Allred[61] that has been used here is based on a quite accurate, semiempirical formula for dissociation energies, namely

$$(\chi_A - \chi_B)^2 = E_d(AB) - \frac{E_d(AA) + E_d(BB)}{2} \quad (7)$$

This illustrates that the square of the difference in the electronegativities takes the deviation from a purely ionic interaction in a compound crystal into account. It is in fact true that the stronger polarizability of "soft" anions has already been used to explain the higher ion mobility in chalcogenides containing sulfur and selenide in comparison to oxides,[13] with their softness reflected in the lower electronegativities of sulfur

https://doi.org/10.1021/jacsau.1c00505
JACS Au 2022, 2, 463−471

and selenide.[62,63] Still, this notion had not been transferred into any descriptor concept before.

The fact that the migration parameter including $\Delta\chi^2$ yields such a good descriptor for the height of the migration barriers reconfirms that a purely ionic consideration of ion mobility in crystals does not capture all factors determining this mobility. It also means that this deviation from ionicity is the reason for the observed nonmonotonic behavior of the migration barriers as a function of the ionic radii, which is correctly taken into account by including the factor $\Delta\chi^2$ in the migration parameter. It is also important to stress the fact that the parameters entering the migration number are basically independent of the particular structure of the considered host lattice, as they correspond to general atomic and ionic properties of the particular elements. The same parameters enter the scaling relations for binaries, spinels, and olivines, confirming the general fundamental nature of the scaling relations.

Note that the linear scaling relations as a function of the migration parameter established in our work do not allow the quantitative prediction of the height of migration barriers in any particular system without any initially measured or calculated data. Thus, they do not correspond to a parametrization of the barrier height as a function of input parameter across all families of possible structures. However, these scaling relations allow us to make qualitative predictions of the height of migration barriers, and once some migration barriers are known in these structures, then even semiquantitative predictions based on easily accessible materials parameters can be made. This will be very beneficial for the identification of promising candidate materials with improved mobility properties. Of course, this linear scaling is not perfect, and we already identified some outliers. Note furthermore that we have concentrated on the vacancy diffusion mechanism in this study, whereas ion migration in crystalline solids can also occur via direct, concerted, or correlated interstitial diffusion. Yet, our descriptor is based on a strict physicochemical reasoning with respect to the interaction strength between the host lattice and the migrating ion plus size arguments by taking ion radii, oxidation states, and the deviation from purely ionic interactions via the difference in the electronegativities into account. These factors should play a role in almost any diffusion mechanism; therefore, deviations from the scaling relations should point to some interesting additional factors also influencing the ion migration and thus to an enhanced fundamental understanding of ion mobility.

Interestingly enough, preliminary results of our group indicate that the ion mobility in the chevrel phase is dominated by size effects.[64] These materials consist of isolated molybdenum octahedra surrounded by chalcogenide atoms.[65] Due to the presence of these stable, quasi-isotropic molecular clusters, there is apparently a different balance of the factors influencing the barrier heights in comparison to that for the more compact binary, ternary, and quaternary materials considered in the study presented here, which, however, are representative for a broad range of solid ionic conductors.

CONCLUSIONS AND SUMMARY

In summary, we propose a descriptor called migration parameter for the ion mobility in crystalline solids that is based on well-accessible materials parameters: namely, ion sizes, oxidation states, and the Pauling electronegativity difference between anions and cations in the compounds. Thus, in contrast to previous attempts to derive descriptors for the ion mobility, we also take the deviation from ionic bonding in the compounds into account. For a broad range of materials classes, we have shown that the height of the migration barrier follows linear scaling relations as a function of this descriptor upon both the variation of the cation chemistry of the migrating ion as well as upon variation of the anion chemistry of the host lattice. This demonstrates the strong predictive power of the descriptor, which should accelerate the discovery of materials with improved migration properties in electrochemical energy storage and conversion.

ASSOCIATED CONTENT

Supporting Information

The Supporting Information is available free of charge at https://pubs.acs.org/doi/10.1021/jacsau.1c00505.

Additional information about details of the density functional theory calculations and the statistical compressed-sensing approach also used to identify possible descriptors (PDF)

AUTHOR INFORMATION

Corresponding Authors

Mohsen Sotoudeh − *Institute of Theoretical Chemistry, Ulm University, 89081 Ulm, Germany;* orcid.org/0000-0002-0970-5336; Email: mohsen.sotoudeh@uni-ulm.de

Axel Groß − *Institute of Theoretical Chemistry, Ulm University, 89081 Ulm, Germany; Helmholtz Institute Ulm (HIU) for Electrochemical Energy Storage, 89069 Ulm, Germany;* orcid.org/0000-0003-4037-7331; Email: axel.gross@uni-ulm.de

Complete contact information is available at: https://pubs.acs.org/10.1021/jacsau.1c00505

Author Contributions

A.G. designed and supervised the whole project. M.S. developed the conceptual framework of the project, performed all calculations, and wrote the first draft of the manuscript. Both authors revised the manuscript and have approved the submitted version.

Notes

The authors declare no competing financial interest.

ACKNOWLEDGMENTS

Useful discussions with Jürgen Janek, University of Gießen, and Holger Euchner, Helmholtz-Institute Ulm, are gratefully acknowledged. This work contributes to the research performed at CELEST (Center for Electrochemical Energy Storage Ulm-Karlsruhe) and was funded by the German Research Foundation (DFG) under Project ID 390874152 (POLiS Cluster of Excellence). Further support by the Dr. Barbara Mez-Starck Foundation and computer time provided by the state of Baden-Württemberg through bwHPC and the German Research Foundation (DFG) through grant no INST 40/575-1 FUGG (JUSTUS 2 cluster) are gratefully acknowledged.

REFERENCES

(1) Choi, S.; Wang, G. Advanced Lithium-Ion Batteries for Practical Applications: Technology, Development, and Future Perspectives. *Adv. Mater. Technol.* **2018**, *3*, 1700376.

(2) Ma, Y.; Ma, Y.; Giuli, G.; Euchner, H.; Groß, A.; Lepore, G. O.; d'Acapito, F.; Geiger, D.; Biskupek, J.; Kaiser, U.; Schütz, H. M.; Carlsson, A.; Diemant, T.; Behm, R. J.; Kuenzel, M.; Passerini, S.;

Bresser, D. Introducing Highly Redox-Active Atomic Centers into Insertion-Type Electrodes for Lithium-Ion Batteries. *Adv. Energy Mater.* **2020**, *10*, 2000783.
(3) Arroyo-de Dompablo, M. E.; Ponrouch, A.; Johansson, P.; Palacín, M. R. Achievements, Challenges, and Prospects of Calcium Batteries. *Chem. Rev.* **2020**, *120*, 6331−6357.
(4) Rajagopalan, R.; Tang, Y.; Ji, X.; Jia, C.; Wang, H. Advancements and Challenges in Potassium Ion Batteries: A Comprehensive Review. *Adv. Funct. Mater.* **2020**, *30*, 1909486.
(5) Elia, G. A.; Marquardt, K.; Hoeppner, K.; Fantini, S.; Lin, R.; Knipping, E.; Peters, W.; Drillet, J.-F.; Passerini, S.; Hahn, R. An Overview and Future Perspectives of Aluminum Batteries. *Adv. Mater.* **2016**, *28*, 7564−7579.
(6) Anji Reddy, M.; Helen, M.; Groß, A.; Fichtner, M.; Euchner, H. Insight into Sodium Insertion and the Storage Mechanism in Hard Carbon. *ACS Energy Lett.* **2018**, *3*, 2851−2857.
(7) Hwang, J.-Y.; Myung, S.-T.; Sun, Y.-K. Sodium-ion batteries: present and future. *Chem. Soc. Rev.* **2017**, *46*, 3529−3614.
(8) Yabuuchi, N.; Kubota, K.; Dahbi, M.; Komaba, S. Research Development on Sodium-Ion Batteries. *Chem. Rev.* **2014**, *114*, 11636−11682.
(9) Gregory, T. D.; Hoffman, R. J.; Winterton, R. C. Nonaqueous Electrochemistry of Magnesium: Applications to Energy Storage. *J. Electrochem. Soc.* **1990**, *137*, 775−780.
(10) Aurbach, D.; Lu, Z.; Schechter, A.; Gofer, Y.; Gizbar, H.; Turgeman, R.; Cohen, Y.; Moshkovich, M.; Levi, E. Prototype systems for rechargeable magnesium batteries. *Nature* **2000**, *407*, 724−727.
(11) MacLaughlin, C. M. Status and Outlook for Magnesium Battery Technologies: A Conversation with Stan Whittingham and Sarbajit Banerjee. *ACS Energy Lett.* **2019**, *4*, 572−575.
(12) Davidson, R.; Verma, A.; Santos, D.; Hao, F.; Fincher, C. D.; Zhao, D.; Attari, V.; Schofield, P.; Van Buskirk, J.; Fraticelli-Cartagena, A.; Alivio, T. E. G.; Arroyave, R.; Xie, K.; Pharr, M.; Mukherjee, P. P.; Banerjee, S. Mapping mechanisms and growth regimes of magnesium electrodeposition at high current densities. *Mater. Horiz.* **2020**, *7*, 843−854.
(13) Maroni, F.; Dongmo, S.; Gauckler, C.; Marinaro, M.; Wolfahrt-Mehrens, M. Through the Maze of Multivalent-ion Batteries: A Critical Review on the status of the research on cathode materials for Mg^{2+} and Ca^{2+} ions insertion. *Batteries Supercaps* **2021**, *4*, 1221−1251.
(14) Singh, N.; Arthur, T. S.; Ling, C.; Matsui, M.; Mizuno, F. A high energy-density tin anode for rechargeable magnesium-ion batteries. *Chem. Commun.* **2013**, *49*, 149−151.
(15) Zhao-Karger, Z.; Gil Bardaji, M. E.; Fuhr, O.; Fichtner, M. A new class of non-corrosive, highly efficient electrolytes for rechargeable magnesium batteries. *J. Mater. Chem. A* **2017**, *5*, 10815−10820.
(16) Aurbach, D.; Cohen, Y.; Moshkovich, M. The Study of Reversible Magnesium Deposition by In Situ Scanning Tunneling Microscopy. *Electrochem. Solid-State Lett.* **2001**, *4*, A113.
(17) Matsui, M. Study on electrochemically deposited Mg metal. *J. Power Sources* **2011**, *196*, 7048−7055.
(18) Zhao, Q. S.; NuLi, Y. N.; Guo, Y. S.; Yang, J.; Wang, J. L. Reversibility of electrochemical magnesium deposition from tetrahydrofuran solutions containing pyrrolidinyl magnesium halide. *Electrochim. Acta* **2011**, *56*, 6530.
(19) Jäckle, M.; Groß, A. Microscopic properties of lithium, sodium, and magnesium battery anode materials related to possible dendrite growth. *J. Chem. Phys.* **2014**, *141*, 174710.
(20) Jäckle, M.; Helmbrecht, K.; Smits, M.; Stottmeister, D.; Groß, A. Self-diffusion barriers: Possible descriptors for dendrite growth in batteries? *Energy Environ. Sci.* **2018**, *11*, 3400−3407.
(21) Janek, J.; Zeier, W. G. A solid future for battery development. *Nature Energy* **2016**, *1*, 16141.
(22) Ikeda, S.; Takahashi, M.; Ishikawa, J.; Ito, K. Solid electrolytes with multivalent cation conduction. 1. Conducting species in Mg-Zr-PO_4 system. *Solid State Ionics* **1987**, *23*, 125−129.
(23) Halim, Z.; Adnan, S.; Mohamed, N. Effect of sintering temperature on the structural, electrical and electrochemical properties of novel $Mg_{0.5}Si_2(PO_4)_3$ ceramic electrolytes. *Ceram. Int.* **2016**, *42*, 4452−4461.
(24) Mohtadi, R.; Matsui, M.; Arthur, T. S.; Hwang, S.-J. Magnesium Borohydride: From Hydrogen Storage to Magnesium Battery. *Angew. Chem., Int. Ed.* **2012**, *51*, 9780−9783.
(25) Unemoto, A.; Matsuo, M.; Orimo, S.-i. Complex Hydrides for Electrochemical Energy Storage. *Adv. Funct. Mater.* **2014**, *24*, 2267−2279.
(26) Higashi, S.; Miwa, K.; Aoki, M.; Takechi, K. A novel inorganic solid state ion conductor for rechargeable Mg batteries. *Chem. Commun.* **2014**, *50*, 1320−1322.
(27) Canepa, P.; Bo, S.-H.; Sai Gautam, G.; Key, B.; Richards, W. D.; Shi, T.; Tian, Y.; Wang, Y.; Li, J.; Ceder, G. High magnesium mobility in ternary spinel chalcogenides. *Nat. Commun.* **2017**, *8*, 1759.
(28) Dillenz, M.; Sotoudeh, M.; Euchner, H.; Groß, A. Screening of Charge Carrier Migration in the $MgSc_2Se_4$ Spinel Structure. *Front. Energy Res.* **2020**, *8*, 260.
(29) Bachman, J. C.; Muy, S.; Grimaud, A.; Chang, H.-H.; Pour, N.; Lux, S. F.; Paschos, O.; Maglia, F.; Lupart, S.; Lamp, P.; Giordano, L.; Shao-Horn, Y. Inorganic Solid-State Electrolytes for Lithium Batteries: Mechanisms and Properties Governing Ion Conduction. *Chem. Rev.* **2016**, *116*, 140−162.
(30) Rong, Z.; Malik, R.; Canepa, P.; Sai Gautam, G.; Liu, M.; Jain, A.; Persson, K.; Ceder, G. Materials Design Rules for Multivalent Ion Mobility in Intercalation Structures. *Chem. Mater.* **2015**, *27*, 6016−6021.
(31) Euchner, H.; Chang, J. H.; Groß, A. On stability and kinetics of Li-rich transition metal oxides and oxyfluorides. *J. Mater. Chem. A* **2020**, *8*, 7956−7967.
(32) Levi, E.; Gofer, Y.; Aurbach, D. On the Way to Rechargeable Mg Batteries: The Challenge of New Cathode Materials. *Chem. Mater.* **2010**, *22*, 860−868.
(33) Huie, M. M.; Bock, D. C.; Takeuchi, E. S.; Marschilok, A. C.; Takeuchi, K. J. Cathode materials for magnesium and magnesium-ion based batteries. *Coord. Chem. Rev.* **2015**, *287*, 15−27.
(34) Verma, V.; Kumar, S.; Manalastas, W., Jr.; Satish, R.; Srinivasan, M. Progress in Rechargeable Aqueous Zinc- and Aluminum-Ion Battery Electrodes: Challenges and Outlook. *Adv. Sustainable Syst.* **2019**, *3*, 1800111.
(35) Yang, T.-Y.; Gregori, G.; Pellet, N.; Grätzel, M.; Maier, J. The Significance of Ion Conduction in a Hybrid Organic−Inorganic Lead-Iodide-Based Perovskite Photosensitizer. *Angew. Chem., Int. Ed.* **2015**, *54*, 7905−7910.
(36) Ghiringhelli, L. M.; Vybiral, J.; Levchenko, S. V.; Draxl, C.; Scheffler, M. Big Data of Materials Science: Critical Role of the Descriptor. *Phys. Rev. Lett.* **2015**, *114*, 105503.
(37) Isayev, O.; Oses, C.; Toher, C.; Gossett, E.; Curtarolo, S.; Tropsha, A. Universal fragment descriptors for predicting properties of inorganic crystals. *Nat. Commun.* **2017**, *8*, 15679.
(38) Nørskov, J. K.; Rossmeisl, J.; Logadottir, A.; Lindqvist, L.; Kitchin, J. R.; Bligaard, T.; Jónsson, H. Origin of the Overpotential for Oxygen Reduction at a Fuel-Cell Cathode. *J. Phys. Chem. B* **2004**, *108*, 17886−17892.
(39) Man, I. C.; Su, H.-Y.; Calle-Vallejo, F.; Hansen, H. A.; Martinez, J. I.; Inoglu, N. G.; Kitchin, J.; Jaramillo, T. F.; Nørskov, J. K.; Rossmeisl, J. Universality in Oxygen Evolution Electrocatalysis on Oxide Surfaces. *ChemCatChem.* **2011**, *3*, 1159−1165.
(40) Wang, Y.; Richards, W. D.; Ong, S. P.; Miara, L. J.; Kim, J. C.; Mo, Y.; Ceder, G. Design principles for solid-state lithium superionic conductors. *Nat. Mater.* **2015**, *14*, 1026.
(41) Muy, S.; Bachman, J. C.; Giordano, L.; Chang, H.-H.; Abernathy, D. L.; Bansal, D.; Delaire, O.; Hori, S.; Kanno, R.; Maglia, F.; Lupart, S.; Lamp, P.; Shao-Horn, Y. Tuning mobility and stability of lithium ion conductors based on lattice dynamics. *Energy Environ. Sci.* **2018**, *11*, 850−859.
(42) Gordiz, K.; Muy, S.; Zeier, W. G.; Shao-Horn, Y.; Henry, A. Enhancement of ion diffusion by targeted phonon excitation. *Cell Reports Physical Science* **2021**, *2*, 100431.

https://doi.org/10.1021/jacsau.1c00505
JACS Au 2022, 2, 463−471

(43) Henß, A.-K.; Sakong, S.; Messer, P. K.; Wiechers, J.; Schuster, R.; Lamb, D. C.; Groß, A.; Wintterlin, J. Density fluctuations as door-opener for diffusion on crowded surfaces. *Science* **2019**, *363*, 715−718.
(44) Henkelman, G.; Jónsson, H. Improved tangent estimate in the nudged elastic band method for finding minimum energy paths and saddle points. *J. Chem. Phys.* **2000**, *113*, 9978.
(45) Kresse, G.; Furthmüller, J. Efficient iterative schemes for ab initio total-energy calculations using a plane-wave basis set. *Phys. Rev. B* **1996**, *54*, 11169−11186.
(46) Blöchl, P. E. Projector augmented-wave method. *Phys. Rev. B* **1994**, *50*, 17953−17979.
(47) Perdew, J. P.; Burke, K.; Ernzerhof, M. Generalized Gradient Approximation Made Simple. *Phys. Rev. Lett.* **1996**, *77*, 3865−3868.
(48) Strauss, E.; Menkin, S.; Golodnitsky, D. On the way to high-conductivity single lithium-ion conductors. *J. Solid State Electrochem.* **2017**, *21*, 1879−1905.
(49) Chen, T.; Sai Gautam, G.; Canepa, P. Ionic Transport in Potential Coating Materials for Mg Batteries. *Chem. Mater.* **2019**, *31*, 8087−8099.
(50) Sotoudeh, M.; Dillenz, M.; Groß, A. Mechanism of Magnesium Transport in Spinel Chalcogenides. *Adv. Energy Sustainability Res.* **2021**, *2*, 2100113.
(51) Allen, L. C.; Capitani, J. F.; Kolks, G. A.; Sproul, G. D. Van Arkel—Ketelaar triangles. *J. Mol. Struct.* **1993**, *300*, 647−655.
(52) Seijo, L.; Barandiaran, Z.; Huzinaga, S. Ab initio model potential study of the equilibrium geometry of alkaline earth dihalides: MX_2 (M = Mg, Ca, Sr, Ba; X = F, Cl, Br, I). *J. Chem. Phys.* **1991**, *94*, 3762−3773.
(53) Ouyang, R.; Curtarolo, S.; Ahmetcik, E.; Scheffler, M.; Ghiringhelli, L. M. SISSO: A compressed-sensing method for identifying the best low-dimensional descriptor in an immensity of offered candidates. *Phys. Rev. Materials* **2018**, *2*, 083802.
(54) Bayliss, R. D.; Key, B.; Sai Gautam, G.; Canepa, P.; Kwon, B. J.; Lapidus, S. H.; Dogan, F.; Adil, A. A.; Lipton, A. S.; Baker, P. J.; Ceder, G.; Vaughey, J. T.; Cabana, J. Probing Mg Migration in Spinel Oxides. *Chem. Mater.* **2020**, *32*, 663−670.
(55) Hörmann, N.; Groß, A. Stability, composition and properties of Li_2FeSiO_4 surfaces studied by DFT. *J. Solid State Electrochem.* **2014**, *18*, 1401−1413.
(56) Fang, M.; Yao, X.; Li, W.; Li, Y.; Shui, M.; Shu, J. The investigation of lithium doping perovskite oxide $LiMnO_3$ as possible LIB anode material. *Ceram. Int.* **2018**, *44*, 8223−8231.
(57) Yu, M.; Trinkle, D. R. Accurate and efficient algorithm for Bader charge integration. *J. Chem. Phys.* **2011**, *134*, 064111.
(58) Tang, W.; Sanville, E.; Henkelman, G. A grid-based Bader analysis algorithm without lattice bias. *J. Phys.: Condens. Matter* **2009**, *21*, 084204.
(59) Wiberg, K. B.; Rablen, P. R. Comparison of atomic charges derived via different procedures. *J. Comput. Chem.* **1993**, *14*, 1504−1518.
(60) De Proft, F.; Van Alsenoy, C.; Peeters, A.; Langenaeker, W.; Geerlings, P. Atomic charges, dipole moments, and Fukui functions using the Hirshfeld partitioning of the electron density. *J. Comput. Chem.* **2002**, *23*, 1198−1209.
(61) Allred, A. Electronegativity values from thermochemical data. *J. Inorg. Nucl. Chem.* **1961**, *17*, 215−221.
(62) Liu, M.; Jain, A.; Rong, Z.; Qu, X.; Canepa, P.; Malik, R.; Ceder, G.; Persson, K. A. Evaluation of sulfur spinel compounds for multivalent battery cathode applications. *Energy Environ. Sci.* **2016**, *9*, 3201−3209.
(63) Mao, M.; Ji, X.; Hou, S.; Gao, T.; Wang, F.; Chen, L.; Fan, X.; Chen, J.; Ma, J.; Wang, C. Tuning Anionic Chemistry To Improve Kinetics of Mg Intercalation. *Chem. Mater.* **2019**, *31*, 3183−3191.
(64) Helmbrecht, K.; Euchner, H.; Groß, A. Impact of dispersion corrections on the properties of Mo_6S_8 for cathode applications. *ChemRxiv, Preprint* 2021. DOI: 10.26434/chemrxiv-2021-d77zd.
(65) Pena, O. Chevrel phases: Past, present and future. *Physica C* **2015**, *514*, 95−112.

https://doi.org/10.1021/jacsau.1c00505
JACS Au 2022, 2, 463−471